

**Dear Topical Editor and Reviewers:**

On behalf of my co-authors, we thank you very much for reviewing our manuscript and giving us a lot of useful comments and suggestions. We appreciate the comments on our manuscript entitled “1 km annual forest cover and plant functional types dataset for China from 1981 to 2023” (Revised version; originally titled: 1 km annual forest cover and plant functional types dataset for China from 1980 to 2023)” (essd-2025-475).

We have revised the manuscript carefully according to the comments. All the changes in the revised manuscript are marked in **red**. And the point-by-point response to the comments of the reviewers is also listed below.

Looking forward to hearing from you soon.

Best regards,

Bo Liu

School of Geography and Tourism, Shaanxi Normal University

No. 620, West Chang'an Street, Chang'an District, Xi'an 710119, China

## **Response to comments**

**Paper: essd-2025-475**

**Title:** 1 km annual forest cover and plant functional types dataset for China from 1981 to 2023

(Revised version; originally titled: 1 km annual forest cover and plant functional types dataset for China from 1980 to 2023)

**Journal: Earth System Science Data**

We sincerely appreciate the reviewers' insightful comments and constructive feedback on our manuscript entitled "1 km annual forest cover and plant functional types dataset for China from 1981 to 2023" (Revised version; originally titled: 1 km annual forest cover and plant functional types dataset for China from 1980 to 2023). We have carefully considered each comment and revised the manuscript accordingly. A point-by-point response to each comment is provided below.

For clarity, our responses are marked in blue, while changes to the text in the revised manuscript are marked in red. Please note that all line numbers refer to the latest revised version of the manuscript uploaded to the system.

### **Response to the Reviewers #1**

**RC1:** Comment on essd-2025-475

This study used multi-source LULC products and provincial-level statistics data to generate a long-term forest cover data, significantly improving the performance of LPJ-GUESS. It's very interesting for your long-term PFTs product and its potential application. I like your detailed method instructions and your reports for the accuracy and comparison of this product.

**Response:** We appreciate your positive assessment of our work. We sincerely thank you for the time and effort you dedicated to a thorough review of this manuscript; your feedback has been clearly helpful in improving its quality. Our point-by-point responses to your comments are provided below:

**[Major Comment 1]** You mentioned the definition of forest cover varies across different LULC products in Table 2. What's your definition of "forest cover" in your study? The "forest consistency" is only an indicator for the forest cover detection, not for the definition in the product.

**Response:** We appreciate this comment. In our study, the definition of "forest cover" adheres to a specific hierarchical classification system. Specifically, the "forest" reconstructed in this study aligns

with the definition of “wooded land” as outlined in China’s Technical Regulations for Continuous Forest Inventory (GB/T 38590-2020). It is defined as: “natural and artificial forests with a canopy cover exceeding 20%”. This category includes arbor forests, economic forests, and other forest tracts (see Table S2 in the Supplement). Furthermore, the definition of PFTs reconstructed in this study follows the definition of “arbor forest” in the same regulations: “Forests composed of arbor tree species with a canopy cover exceeding 20%”, as well as its subordinate hierarchical classifications (for details, see Table S2). These definitions are crucial for establishing area constraints for each forest category and for harmonizing the mapping of “forest” classes across multi-source Land Use and Land Cover (LULC) products (i.e., the potential forest cover areas in this study).

During the forest reconstruction process, we applied the “wooded land” area constraint derived from provincial National Forest Inventory (NFI) data, a category that explicitly excludes shrublands (Table S2). Consequently, when extracting forest data from multi-source LULC products, we selected only those class values that are strictly or substantially consistent with the definition of “wooded land”: For example, for CNLUCC, we selected the category with value 21 (“Wooded Land”) as potential forest pixels. We did not select the broader value 2 (“Forest”) because it includes sub-categories such as value 22 (“Shrubland”) and value 23 (“Sparse Woods”), which do not align with our study’s definition. For GLC\_FCS30D, we selected categories with values 51–92 (Evergreen Needleleaf, Evergreen Broadleaf, Deciduous Needleleaf, Deciduous Broadleaf, and Mixed leaf forests) and excluded values 120–122 (Shrub categories). This logic was consistently applied to all other LULC products. This approach maximizes the consistency between the forest categories selected from multi-source LULC data and the area constraints derived from NFI data. It thereby ensures the accuracy of the subsequent step, where NFI forest areas are allocated to potential forest grids based on consistency levels.

Regarding PFT classification, we utilized the definition and area of “arbor forest” as the constraint. This category includes both needleleaf and broadleaf forests, and its total area is strictly less than that of “wooded land”. Under this definition, the reconstructed extent of needleleaf and broadleaf forests will not exceed the extent of the reconstructed forest, which serves as the prerequisite for our subsequent PFT pixel allocation method.

We have added a new section, **Section 3.1: Definition of forest**, to systematically describe this

process (**Page 7, Lines 179–195 of the revised manuscript**). Furthermore, in accordance with these definitions, the entire **Section 3 (Methods)** has been revised to ensure consistency. For the complete content, please refer to the “Methods” section in the revised manuscript.

**[Major Comment 2]** The maximum NDVI values were applied to detecting potential forest cover and PFTs. However, maximum NDVI is unstable due to the interference of clouds, especially in those cloudy area.

**Response:** In our original manuscript, we utilized the dataset developed by Jeong et al. (2024). A critical step in that dataset’s generation was the application of the HANTS (Harmonic Analysis of Time Series) method during preprocessing. HANTS is a time-series reconstruction technique that effectively identifies and interpolates missing data or low values caused by cloud contamination. Consequently, the original monthly NDVI data provided a reconstructed, smoothed, and clean time series. Given the absence of cloud interference in this dataset, the use of the maximum value composite (MVC) method was initially considered reasonable.

However, a significant limitation of that dataset is its native resolution of 0.05°. Even after resampling it to 1 km, we observed that the forest cover maps reconstructed using this data exhibited “coarse grid artifacts” in certain regions. Unfortunately, no alternative NDVI datasets with a resolution higher than 1 km are currently available for the 1980s. Therefore, in the revised manuscript, we adopted the China 1985–2023 Annual Landsat Composite Dataset published by Cai et al. (2025). This dataset integrates imagery from multiple Landsat sensors and addresses critical issues such as cloud and shadow contamination, reflectance consistency, and data gaps. Specifically, because this dataset employs a median composite method to aggregate all images from the annual growing season into a single annual image, we directly calculated the annual NDVI for the 1985–2023 period using the Red and Near-Infrared (NIR) bands. We then resampled these data to match our target resolution using the mean method. Due to the scarcity of Landsat imagery in the early 1980s, we used the 1985 data as a proxy for the 1981–1984 period. By utilizing this higher-resolution dataset, the issue of coarse grid artifacts has been effectively resolved. We have revised **Section 2.3: Satellite-based vegetation index dataset (Page 5, Lines 137–147)** to align with our modifications.

**References:**

Cai, Y., Li, X., Zhu, P., Nie, S., Wang, C., Liu, X., and Chen, Y.: China Earth Observation Data Cube:

The 30-m Seamless Annual Leaf-On Landsat Composites from 1985 to 2023, *J. Remote Sens.*, 5, 0698, <https://doi.org/10.34133/remotesensing.0698>, 2025.

Jeong, S., Ryu, Y., Gentine, P., Lian, X., Fang, J., Li, X., Dechant, B., Kong, J., Choi, W., and Jiang, C.: Persistent global greening over the last four decades using novel long-term vegetation index data with enhanced temporal consistency, *Remote Sens. Environ.*, 311, 114282, <https://doi.org/10.1016/j.rse.2024.114282>, 2024.

**[Major Comment 3]** During the process of PFTs classification, you aggregated a mass of distinct data layers from 1980 to 2013 for two or four consistency maps and used it to classify PFTs in each year. Is it reasonable to consider information from 1980 to 2013 when you were detecting PFTs in 1980? For example, if the broadleaf forest turned into needleleaf forest in 1985, will it be recognized as needleleaf in 1980? I understand you have assumed that the relative spatial distribution of PFTs remains static, but i m not sure whether it is reasonable.

**Response:** We appreciate your valuable feedback and fully acknowledge the importance of accounting for potential temporal changes in PFTs. Regarding the potential transitions between broadleaf and needleleaf forests, we have conducted an in-depth analysis to address this concern:

First, we quantitatively assessed the actual scale of these PFT transitions using the GLC\_FCS30D, MCD12Q1, and ESA CCI datasets. Taking GLC\_FCS30D as an example, we extracted pixels classified as broadleaf (value 51–62) and needleleaf (value 71–82) in both 1985 and 1990. Our comparative analysis revealed that pixels transitioning from broadleaf to needleleaf (or vice versa) over this five-year period accounted for only 0.17% of the total needleleaf and broadleaf pixels in 1990 (see **Table S4 in the Supplement**). Similarly, transition rates in ESA CCI (0.00%) and MCD12Q1 (0.34%) were negligible (**Table S4**). This extremely low proportion indicates that mutual transitions between these two major forest types are very rare, even over a five-year span. When aggregated to the 1 km resolution used in this study, such minor variations (<0.34%) become virtually negligible during the spatial aggregation process. Therefore, at the macro scale (1 km), the impact of needleleaf-broadleaf transitions on our study is minimal.

Furthermore, our hypothesis is supported by a solid ecological foundation. As the two primary forest types, the large-scale distributions of needleleaf and broadleaf forests are predominantly controlled by relatively stable long-term climatic, edaphic, and topographic conditions, collectively

referred to as their respective ecological niches (Fragnière et al., 2015; Steidinger et al., 2019). Within the 1981–2023 timeframe, while localized land use changes (e.g., logging) or natural disturbances (e.g., fire, pests) may cause short-term PFT fluctuations, the climatic niches driving their macro-distribution remain relatively constant at the national scale. For instance, broadleaf forests typically require longer growing seasons and warmer temperatures, whereas needleleaf forests are more tolerant of cold and shorter growing seasons. These fundamental niche differences constrain systematic mutual transitions in the absence of significant climate change or large-scale, persistent artificial intervention. Consequently, we consider the probability of large-scale, systematic needleleaf-broadleaf transitions to be very low. Our aggregated consistency maps are designed precisely to capture this dominant spatial pattern determined by climatic niches, rather than annual short-term disturbances.

Nonetheless, we fully acknowledge that aggregating information from 1981–2023 for historical classification represents a simplification assumption. In extreme cases (e.g., where a pixel indeed underwent a type of transition in 1985), our method might misclassify the post-transition state (e.g., 1985) based on the dominant state of 1980. From a remote sensing perspective, accurately monitoring historical needleleaf-broadleaf transitions at the national scale is highly challenging. Prior to the availability of high-resolution Sentinel imagery (10 m) in 2015 (Klehr et al., 2025; Mäyrä et al., 2021), relying on medium-resolution imagery like Landsat made high-precision differentiation difficult, let alone capturing dynamic transitions in specific years. While change detection algorithms for Landsat time series (e.g., LandTrendr, CCDC) exist, they primarily distinguish land cover types based on spectral changes (Pasquarella et al., 2022). Given the high spectral similarity between these two forest types, these algorithms may detect that a forest has “changed” (e.g., reforestation after logging), but it remains extremely difficult to accurately distinguish whether this change represents a transition between needleleaf and broadleaf types or merely disturbance and recovery within the same forest type.

Therefore, we argue that employing consistency maps generated from aggregated, multi-source data is currently the more robust approach for distinguishing these two PFTs over long time series. We have also included a discussion of this point in the revised manuscript (**Page 30, Lines 684–704**).

## **References:**

- Fragnière, Y., Bétrisey, S., Cardinaux, L., Stoffel, M., and Kozłowski, G. J. J.: Fighting their last stand? A global analysis of the distribution and conservation status of gymnosperms, *J. Biogeogr.*, 42, 809–820, <https://doi.org/10.1111/jbi.12480>, 2015.
- Klehr, D., Stoffels, J., Hill, A., Pham, V.-D., van der Linden, S., and Frantz, D.: Mapping tree species fractions in temperate mixed forests using Sentinel-2 time series and synthetically mixed training data, *Remote Sens. Environ.*, 323, 114740, <https://doi.org/10.1016/j.rse.2025.114740>, 2025.
- Mäyrä, J., Keski-Saari, S., Kivinen, S., Tanhuanpää, T., Hurskainen, P., Kullberg, P., Poikolainen, L., Viinikka, A., Tuominen, S., and Kumpula, T.: Tree species classification from airborne hyperspectral and LiDAR data using 3D convolutional neural networks, *Remote Sens. Environ.*, 256, 112322, <https://doi.org/10.1016/j.rse.2021.112322>, 2021.
- Pasquarella, V. J., Arévalo, P., Bratley, K. H., Bullock, E. L., Gorelick, N., Yang, Z., and Kennedy, R. E.: Demystifying LandTrendr and CCDC temporal segmentation, *Int. J. Appl. Earth Obs. Geoinf.*, 110, 102806, <https://doi.org/10.1016/j.jag.2022.102806>, 2022.
- Steidinger, B. S., Crowther, T. W., Liang, J., Van Nuland, M. E., Werner, G. D., Reich, P. B., Nabuurs, G.-J., De-Miguel, S., Zhou, M., and Picard, N.: Climatic controls of decomposition drive the global biogeography of forest-tree symbioses, *Nature*, 569, 404–408, <https://doi.org/10.1038/s41586-019-1128-0>, 2019.

**[Major Comment 4]** Check your total forest area for GLC\_FCS products and other datasets. I calculated the forest cover area from value 51 to 92 derived from GLC\_FCS dataset for China in 2010 using Google Earth Engine, the area was about 240,000,000 ha, not 350,000,000 ha. What's more, Xia et al. also reported that the total forest area for GLC\_FCS products in 2010 is about 220,000,000 ha (Reconstructing Long-Term Forest Cover in China by Fusing National Forest Inventory and 20 Land Use and Land Cover Data Sets, in Figure 7). The accurate total area of forest cover in your product is a significant advantage compare to other products, but your imprecise statistics data make me doubtful.

**Response:** We apologize for this oversight. In our previous calculations of total forest, needleleaf, and broadleaf areas, we utilized the resampled data, which resulted in an overestimation of the forest

area. In the revised manuscript, we have recalculated these figures using the original data (at native resolution). We found that the forest area in the GLC\_FCS30D dataset ranges from 232 to 238 million hectares (Mha) for the period 1985–2022, with a total area of 234 Mha in 2010. We have performed similar recalculations for the other datasets and have revised **Figure 5** accordingly.

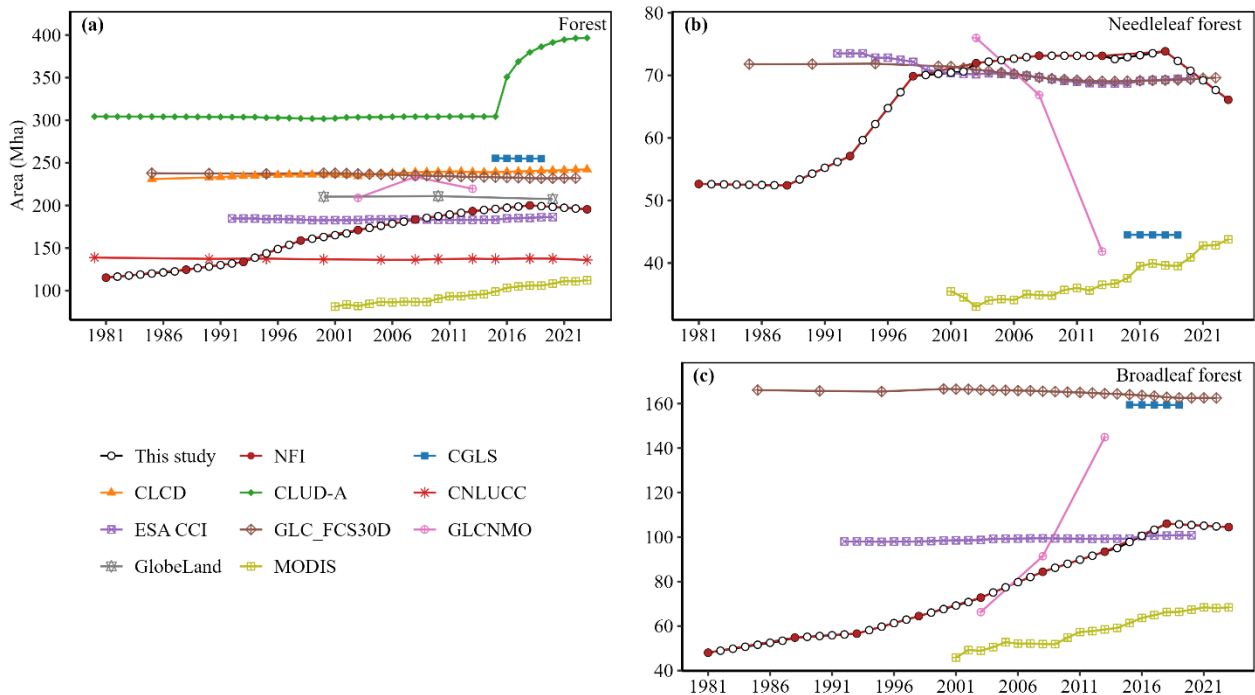


**Figure 5.** Temporal dynamics of national-scale total forest area, comparing the results of this study with data from national forest inventory (NFI) and other selected land use and land cover (LULC) products: (a) forest, (b) needleleaf forest, and (c) broadleaf forest.

**[Major Comment 5]** You used GLC\_FCS30 in 2010 and 2015 as the proxy for LULC maps in 2011 and 2013. However, the annual LULC map from 2000 in GLC\_FCS dataset is available now. You could update your LULC dataset to compare with other forest datasets more accurately. It's necessary to precisely display the accuracy difference among your product and other datasets.

**Response:** We appreciate your feedback. In the revised manuscript, we have updated our validation strategy strictly following the good practice guidelines for sample size decisions proposed by Olofsson et al. (2014). To assess the accuracy of the reconstructed dataset, we utilized independent historical validation samples to validate five forest types—evergreen needleleaf, evergreen broadleaf, deciduous needleleaf, deciduous broadleaf, and mixed leaf Forests—across the entire 1981–2023 period. Furthermore, we conducted a comparative assessment against the GLC\_FCS30D, ESA CCI,

and MCD12Q1 datasets. The results indicate that our dataset achieved a mean overall accuracy (OA) of  $84.86\% \pm 1.18\%$ , which outperforms ESA CCI (mean  $83.47\% \pm 1.15\%$ ), MCD12Q1 (mean  $61.17\% \pm 1.36\%$ ), and the global 30 m land-cover dynamics monitoring dataset (GLC\_FCS30D) (mean  $78.92\% \pm 1.24\%$ ) (**Fig. 2f**). The detailed validation methodology and corresponding figures are presented in the revised manuscript (**Section 3.5, Page 13, Lines 371–408, and Section 4.1, Page 16, Lines 464–474**).

#### **References:**

Olofsson, P., Foody, G. M., Herold, M., Stehman, S. V., Woodcock, C. E., and Wulder, M. A.: Good practices for estimating area and assessing accuracy of land change, *Remote Sens. Environ.*, 148, 42–57, <https://doi.org/10.1016/j.rse.2014.02.015>, 2014.

**[Major Comment 6]** In Fig. S1, the sum of needleleaf forest area and broadleaf forest area is quite different from the total forest area. Why it happened? If there are many mixed leaf forest areas, how to distinguish needleleaf forest or broadleaf forest from the mixed forest? By the way, the legend “BF” and “NF” were not explained in the figure or caption.

**Response:** In the National Forest Inventory (NFI), the “forest area” is composed of needleleaf forests, broadleaf forests, bamboo forests, economic forests, and shrublands (**see Section 3.1, Page 7, Lines 179–195**); consequently, there is a discrepancy between the sum of needleleaf/broadleaf forest areas and the total forest area reported in the NFI. Due to major ecological restoration initiatives such as the Three-North Shelterbelt Program and the Grain for Green Program, extensive afforestation was conducted across China in the early 21st century, particularly in the Northwest. However, owing to the arid and semi-arid climate in these regions, tree survival rates were often low (Li et al., 2021; Zhang et al., 2022), leading national strategies to shift towards planting extensive areas of shrubs to better adapt to local climatic conditions.

Regarding the consistency of forest classification, this prevalence of shrublands can introduce challenges when using the broad NFI “forest area” as a constraint, as it may inadvertently encompass shrub-dominated areas in the Northwest. This factor likely contributes to the differences in consistency patterns observed between our study and previous works (Xia et al., 2023). A distinctive feature of our study is the adoption of “wooded land” (which explicitly excludes shrubland) as the area constraint. This targeted approach effectively minimizes the potential confounding effects of

shrublands on forest identification. Consequently, we observed improved alignment in regions like Xinjiang and Qinghai, with lower consistency remaining primarily in Ningxia (**Page 17, Line 494, Fig. S9**). This strategy also ensures that the sum of our reconstructed needleleaf and broadleaf areas aligns more closely with the target forest area (**Fig. 5**). Accordingly, we have removed the original Figure S1 and replaced it with a figure illustrating the area reconstruction process for “wooded land” (**Revised Fig. S2**). We have also updated **Sections 3.1 and 3.2 (Page 7, Lines 179–226)** of the Methods to provide a systematic description of this process.

Regarding mixed forests, according to China’s *Technical Regulations for Continuous Forest Inventory* (GB/T 38590-2020), mixed needle-broadleaf forests are technically classified within the needleleaf forest category. Therefore, we were able to distinguish mixed forests using an analogous approach to how we differentiate between evergreen and deciduous needleleaf forests. We have introduced a new extraction logic for mixed forests in **Section 3.4.2 (Page 11, Lines 314–352)**, through which these forests have been successfully identified and mapped (**Figure 4**).

#### **References:**

Li, C., Fu, B., Wang, S., Stringer, L. C., Wang, Y., Li, Z., Liu, Y., and Zhou, W.: Drivers and impacts of changes in China’s drylands, *Nat. Rev. Earth Environ.*, 2, 858–873, <https://doi.org/10.1038/s43017-021-00226-z>, 2021.

Xia, X., Xia, J., Chen, X., Fan, L., Liu, S., Qin, Y., Qin, Z., Xiao, X., Xu, W., and Yue, C.: Reconstructing long-term forest cover in China by fusing national forest inventory and 20 land use and land cover data sets, *J. Geophys. Res.-Biogeo.*, 128, e2022JG007101, <https://doi.org/10.1029/2022JG007101>, 2023.

Zhang, L., Sun, P., Huettmann, F., and Liu, S.: Where should China practice forestry in a warming world?, *Glob. Change Biol.*, 28, 2461–2475, <https://doi.org/10.1111/gcb.16065>, 2022.

**[Minor Comment 1]** You used the different hyphen in the manuscript. In line 8 and 23, “long-term” and “long–term”, make the format consistent.

**Response:** We appreciate this suggestion. We agree that the correct form is “long-term”, and we have revised **Line 24** in the revised manuscript (originally Line 23) accordingly. Additionally, we have thoroughly checked the entire manuscript to ensure the consistent and correct use of hyphens throughout the text:

*“With its high spatial resolution, long-term temporal coverage, and detailed forest-type classification, ...”*

**[Minor Comment 2]** In line 85, “every several year” is confusing.

**Response:** The correct form is “every few years”. Thank you for the correction.

**[Minor Comment 3]** In the resampling process, you used the nearest neighbor method. Why don’t use the mode of LULC type?

**Response:** You are correct. Nearest neighbor resampling assigns the new pixel value based directly on the value of the pixel closest to the center in the original raster. In contrast, mode (majority) resampling determines the new pixel value based on the most frequently occurring value in the original raster. We agree that for the purposes of this study, the mode method is the superior choice. Consequently, we have modified our resampling methodology, which is described on **Page 5, Line 135**. Furthermore, this change is reflected in our newly uploaded dataset, and the statistical results in the revised manuscript have been updated and now differ from the previous version:

*“...(ii) resampling to a 1 km resolution using the majority method...”*

**[Minor Comment 4]** In Fig. 3, you marked the p-value as “P” instead of “p”. This is a mistake. What’s more, the high consistency between NFI forest areas and reconstructed forest areas is obvious owe to your method. Although this figure is delicate, it’s useless in the paper.

**Response:** We appreciate this suggestion. We have revised Figure 3 and re-uploaded it as a supplementary file (Figure S10).

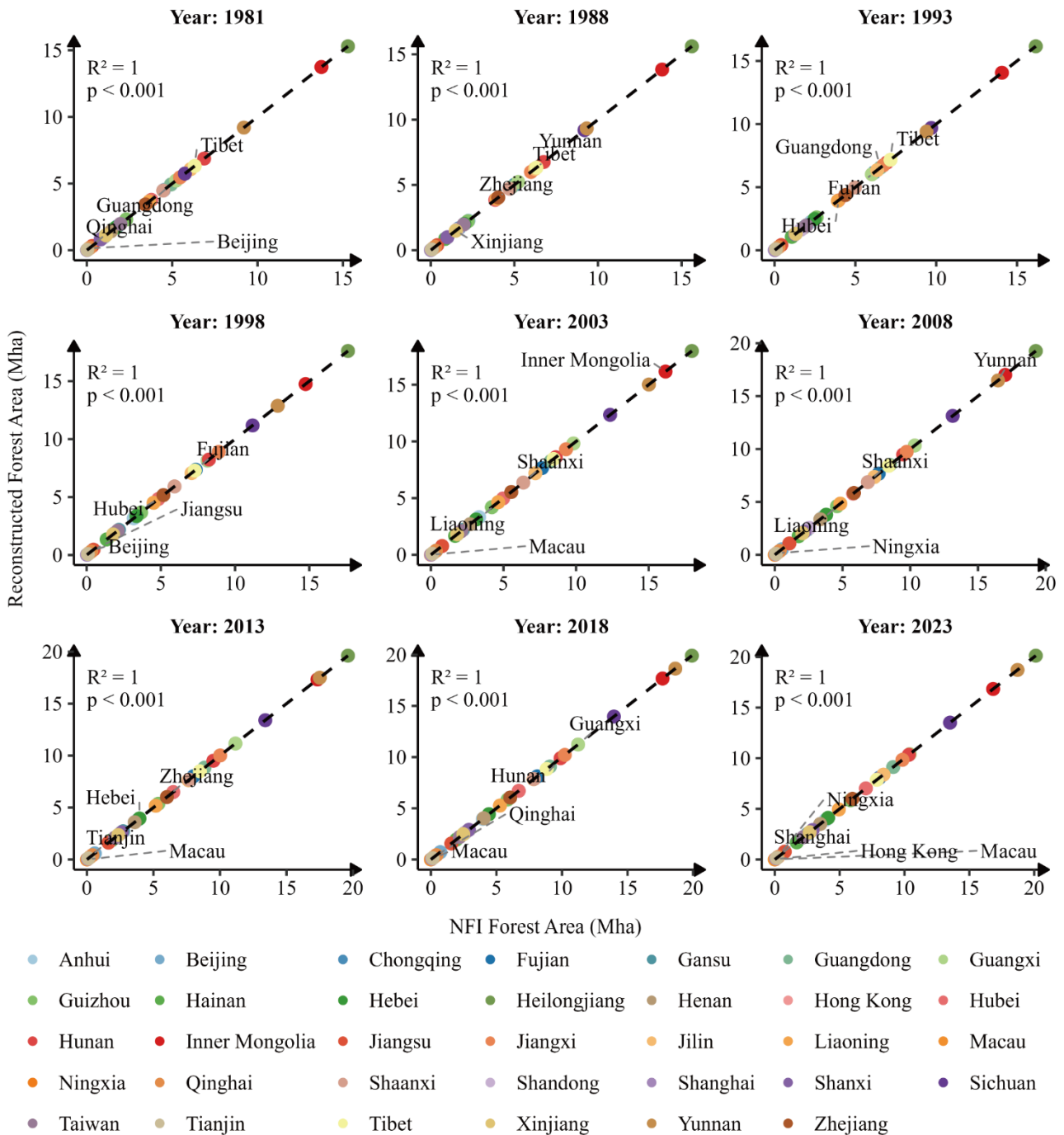


**Figure S10.** Scatter plot comparing provincial-level forest area as reported by the national forest inventory (NFI) with estimates from the reconstructed maps of this study.

**[Minor Comment 5]** You displayed the CLCNMO dataset in Fig. 5 and line 548, but they cannot be found in the Fig. S2, Table S1 and Table S2. Is it CLCNMO or GLCNMO? Check it carefully.

**Response:** We apologize for this error. The correct acronym is GLCNMO. We have corrected the text in the revised manuscript accordingly. Thank you for pointing this out.

We appreciate your warm work earnestly, and hope that the correction will meet with approval. We tried our best to improve the manuscript and made some changes in the manuscript. These changes will not influence the content and framework of the paper. And here we did not list the changes but marked in red in revised paper.

**Once again, thank you very much for your comments and suggestions.**

## **Response to comments**

**Paper: essd-2025-475**

**Title:** 1 km annual forest cover and plant functional types dataset for China from 1981 to 2023

(Revised version; originally titled: 1 km annual forest cover and plant functional types dataset for China from 1980 to 2023)

**Journal: Earth System Science Data**

We sincerely appreciate the reviewers' insightful comments and constructive feedback on our manuscript entitled "1 km annual forest cover and plant functional types dataset for China from 1981 to 2023" (Revised version; originally titled: 1 km annual forest cover and plant functional types dataset for China from 1980 to 2023). We have carefully considered each comment and revised the manuscript accordingly. A point-by-point response to each comment is provided below.

For clarity, our responses are marked in blue, while changes to the text in the revised manuscript are marked in red. Please note that all line numbers refer to the latest revised version of the manuscript uploaded to the system.

## **Response to the Reviewers #2**

**RC2:** Comment on essd-2025-475

This study developed a 1 km resolution annual forest cover dataset (1980–2023) and an 8-class plant functional type (PFT) dataset (1981–2013) by integrating multi-source remote sensing data with National Forest Inventory (NFI) statistics. They aimed to address the critical limitations of existing land cover products—their inability to capture China's forest expansion since the 1980s and the inadequacy of plant functional types data for dynamic global vegetation models (DGVMs). The reliability and applicability of the datasets were validated through field surveys and simulations using the LPJ-GUESS model. The data could provide valuable support for national carbon balance assessments. However, I still have some concerns about the dataset: insufficient novelty in core methods (forest cover reconstruction) relative to existing literature, as well as potential issues with data quality due to incomplete validation and model simulations.

**Response:** We sincerely appreciate the time and effort you have dedicated to a thorough review of this manuscript; your feedback has been instrumental in improving its quality. While we fully

acknowledge your concerns regarding methodological novelty and dataset quality, we would like to take this opportunity to clarify the specific methodological advancements presented in this study and to highlight the extensive validation efforts we have incorporated into the revised manuscript. Our point-by-point responses to your specific comments are provided below:

**[Major Comment 1]** The novelty of the forest cover reconstruction method is limited. Its core logic, integrating NFI statistics with multi-source land cover consistency, closely resembles the approach of Xia et al. (2023). The authors should explicitly acknowledge this overlap and clearly articulate what distinguishes their work, such as extending the temporal coverage to 2023, refining NDVI-based pixel selection, or improving provincial-scale constraint algorithms.

**Response:** We appreciate this constructive comment. We acknowledge that our fundamental logical framework draws inspiration from the methodology of Xia et al. (2023), and we have cited their work extensively throughout the manuscript. However, as per your suggestion, we have significantly optimized and extended this framework to address specific limitations present in their study. The key improvements and distinctions are detailed below:

**1. Stricter definition of NFI constraints.** The core distinction between our work and that of Xia et al. (2023) lies in our stricter definition of the NFI constraint rules. Unlike Xia et al. (2023), who directly utilised the “total forest area” from the NFI as a constraint, we made a clear distinction regarding the definition of forest. In the National Forest Inventory, “total forest area” comprises needleleaf forests, broadleaf forests, bamboo forests, economic forests, and shrublands (see **Section 3.1, Page 7, Lines 179-195**). In our study, we employed the “wooded land” area from the NFI—which explicitly excludes the “shrubland” category—as our total forest constraint. This approach maximizes the semantic consistency between the “potential forest pixels” selected from multi-source LULC products (most of which classify shrubs separately) and the NFI statistical data. This ensures the accuracy of the subsequent step where NFI forest and PFT areas are allocated to potential consistency pixels.

Specifically, due to major ecological restoration initiatives such as the Three-North Shelterbelt Program and the Grain for Green Program, extensive afforestation was conducted across China in the early 21st century, particularly in the Northwest. However, owing to the arid and semi-arid climate in these regions, tree survival rates were often low (Li et al., 2021; Zhang et al., 2022). Consequently,

national strategies shifted towards planting extensive areas of shrubs to better adapt to local climatic conditions. When using the broad NFI “total forest area” as a constraint, this widespread distribution of shrubs poses a challenge, as it can lead to the inadvertent misclassification of shrub-dominated areas in the Northwest as forest.

In contrast, our strict “wooded land” constraint improved classification consistency in Northwest China. While Xia et al. (2023) observed low consistency in Xinjiang, Qinghai, and Ningxia, our study observed low consistency only in Ningxia (**Page 17, Line 494, Fig. S9**). This strict definition also ensured that the sum of our reconstructed needleleaf and broadleaf areas aligns more closely with the total reconstructed forest area (**Fig. 5**).

**2. Granularity and robustness of PFT allocation.** We have improved the PFT allocation method to be both more granular and more robust. Compared to the four core forest types provided by Xia et al. (2023) (evergreen/deciduous needleleaf/broadleaf), our study offers nine PFTs (**see Fig. 4**) that are more suitable for Dynamic Global Vegetation Models (DGVMs). We not only added the mixed leaf forest category but also further distinguished boreal, temperate, and tropical types based on climatic rules. Furthermore, regarding the allocation algorithm, we established a refined, hierarchical logic to handle complex scenarios (**see Section 3.4, Page 9, Lines 255-370**), such as cases where LULC consistency is insufficient (one type is “valid” while the other is “invalid”), where conflicts exist (e.g., “ambiguous” pixels), or where residuals remain (handled via neighbourhood analysis and environmental inference). These refined rules ensure that even when conflicts exist among data sources, the resulting map strictly satisfies the NFI area constraints for needleleaf and broadleaf forests while maintaining a reasonable distribution of PFT subtypes.

**3. Extended temporal resolution and practical utility.** We have extended the temporal coverage to provide annual PFT distributions from 1981 to 2023. As demonstrated in our results, this high temporal resolution is critical for capturing inter-annual forest dynamics and accurately identifying the “onset year” and “duration” of forest change events (**see Section 4.3, Page23, Lines 549-575**), capabilities that multi-year interval products cannot offer. Moreover, as mentioned in the Introduction (**Page3, Lines 72–89**), accurate simulation of forest carbon dynamics and vegetation succession under restoration processes requires DGVMs driven by annually updated PFT data that reflect China’s recent forest recovery. Therefore, our study provides a reliable data foundation for such simulations.

Subsequent comparative analysis using the LPJ-GUESS model against mainstream datasets (see **Section 4.4, Page 25, Lines 576-646**) indicates that compared to ESA CCI PFT and MCD12Q1, our dataset reduces simulation errors for key ecosystem variables (GPP, NEE, LAI, ET) across 63.1%–85.3% of China’s land area (**Fig. 9**). This result demonstrates the practical value of our dataset in improving ecosystem modeling.

#### **References:**

Li, C., Fu, B., Wang, S., Stringer, L. C., Wang, Y., Li, Z., Liu, Y., and Zhou, W.: Drivers and impacts of changes in China’s drylands, *Nat. Rev. Earth Environ.*, 2, 858–873, <https://doi.org/10.1038/s43017-021-00226-z>, 2021.

Xia, X., Xia, J., Chen, X., Fan, L., Liu, S., Qin, Y., Qin, Z., Xiao, X., Xu, W., and Yue, C.: Reconstructing long-term forest cover in China by fusing national forest inventory and 20 land use and land cover data sets, *J. Geophys. Res.-Biogeo.*, 128, e2022JG007101, <https://doi.org/10.1029/2022JG007101>, 2023.

Zhang, L., Sun, P., Huettmann, F., and Liu, S.: Where should China practice forestry in a warming world?, *Glob. Change Biol.*, 28, 2461–2475, <https://doi.org/10.1111/gcb.16065>, 2022.

**[Major Comment 2]** The field-scale validation is inadequate. The manuscript relies heavily on public datasets concentrated in 2011–2015, which does not adequately test the accuracy of the 1980–2010 and 2015-2023 portions of the dataset. Moreover, only broadleaf and needleleaf forest types were validated, whereas at least four types should be assessed given that the PFTs dataset includes eight types. To strengthen credibility, independent and historical validation data are needed, for example through visual interpretation of archived Google Earth imagery to obtain historical records.

**Response:** We sincerely appreciate this crucial suggestion. To address your concerns and strengthen the credibility of our results, we have completely reconstructed the validation framework in the revised manuscript. We adopted a rigorous approach following the good practice guidelines proposed by Olofsson et al. (2014), combining field survey samples, historical Google Earth imagery, and Landsat time series to conduct an independent validation across the entire 1981–2023 period for five key forest types (evergreen needleleaf forest, evergreen broadleaf forest, deciduous needleleaf forest, deciduous broadleaf forest, and mixed leaf forest). The specific improvements are as follows:

**1. Extension of temporal coverage (1981–2023):** As per your suggestion, we moved beyond reliance on single-period NFI data. We implemented a strategy combining ground surveys with dense remote sensing time series to derive reliable historical validation samples: We utilised the LandTrendr algorithm to examine the temporal stability of the NFI ground plot locations (2009–2013) using dense Landsat time series from 1985 to 2023. By identifying “stable” samples (i.e., those that remained unchanged throughout the period) and “unstable” samples (i.e., those that underwent change at least once during the period), we were able to reliably backcast or extrapolate high-quality ground truth labels to the entire study period. For each annual validation set, we conducted manual visual interpretation and verification using high-resolution imagery archived from Google Earth. This extensive effort was carried out by a team of ten experienced remote sensing experts through multiple rounds of cross-validation and discussion, ensuring the accuracy of validation data, particularly for the historical period.

**2. Independent accuracy assessment:** We strictly followed the good practice guidelines for accuracy assessment proposed by Olofsson et al. (2014). This process involved implementing a proportional stratified sampling design, correcting accuracy estimates based on map uncertainty, and calculating the corresponding standard errors and 95% confidence intervals. Furthermore, to comprehensively evaluate the quality of the reconstructed dataset, we conducted a comparative assessment against existing annual land cover products that include the five-plant functional type (PFT) categories (Evergreen Needleleaf, Evergreen Broadleaf, Deciduous Needleleaf, Deciduous Broadleaf, and Mixed leaf Forests)—namely, the ESA CCI, MCD12Q1, and GLC\_FCS30D datasets. In addition to this sample-based validation, we performed an indirect accuracy assessment of the five PFT categories by analyzing the consistency among the input LULC datasets. This approach enables the quantification of classification confidence at the pixel level and spatially reflects the reliability of the reconstruction results (i.e., higher consistency implies a greater likelihood of correct classification), thereby serving as a crucial supplement to sample-based validation.

In summary, our new validation scheme fully leverages historical archived imagery and time-series techniques to resolve the issues of incomplete temporal coverage and insufficient type validation. Detailed descriptions of the methodology and results have been updated in **Section 3.5 (Page 13, Lines 371-413)** and **Section 4.1 (Page 16, Lines 463-507)** of the revised manuscript.

## References:

Olofsson, P., Foody, G. M., Herold, M., Stehman, S. V., Woodcock, C. E., and Wulder, M. A.: Good practices for estimating area and assessing accuracy of land change, *Remote Sens. Environ.*, 148, 42–57, <https://doi.org/10.1016/j.rse.2014.02.015>, 2014.

**[Major Comment 3]** Descriptions of simulation experiments using LPJ-GUESS are not sufficiently clear. (1) The manuscript does not specify the temporal scale of simulations (daily or monthly), which is important for interpreting variables such as GPP. (2) No description about parameter calibration for Chinese forest ecosystems, which likely contributes to questionable outputs. (3) Comparisons are limited to ESA CCI PFTs rather than including higher-resolution datasets (e.g., GLC\_FCS), and the reported anomaly in southern China is presented without explanation.

**Response:** We sincerely appreciate these constructive comments regarding the LPJ-GUESS simulation assessment. We have meticulously revised the manuscript to provide detailed explanations of the simulation setup, parameterization, and dataset comparison process. Our point-by-point responses are as follows:

**1. Regarding the simulation time scale:** We have explicitly stated in **Section 3.7 (Page 15, Lines: 430-461)** that the model is driven by daily meteorological forcing data (CMFD 2.0) to accurately capture vegetation dynamics at the daily scale, while the output variables (Gross Primary Production (GPP), Net Ecosystem Exchange (NEE), Leaf Area Index (LAI), and Evapotranspiration (ET)) are output and analyzed at a monthly time scale. Specifically, for the comparative analysis, we focused on the mean values during the summer season (June–August) to highlight primary physiological activities.

**2. Regarding parameter calibration for Chinese forests and anomalies in Southern China:** We fully acknowledge the importance of parameterization. In the revised manuscript (**Section 3.7**), we have manually adjusted key parameters related to photosynthesis, autotrophic respiration, and plant water use efficiency to better represent Chinese forest ecosystems. The updated Plant Functional Type (PFT) parameters are summarized in **Table S3 of the Supplementary Material**. Through these adjustments, we have mitigated the simulation anomalies originally observed in the forest ecosystems of Southern China.

However, this study did not perform a comprehensive, systematic calibration and optimization

across the entirety of China. This is primarily because disentangling the interacting uncertainties among data inputs, model structure, and climate drivers remains a complex challenge. Given China's vast territory and significant environmental gradients—ranging from arid and semi-arid to humid zones—the dominant ecophysiological processes (e.g., light competition in humid regions versus hydraulic constraints in arid regions) vary substantially across the landscape. Therefore, developing a fine-scale, regionally differentiated parameterization scheme was beyond the scope of this study, though it represents a key direction for our future research. We have elaborated on this in the discussion section (**Page 31 Lines 705-723**).

Furthermore, we wish to emphasize that the core objective of this simulation experiment was to compare the relative impact of different PFT datasets on model outputs, rather than to achieve absolute simulation truth. To isolate the independent influence of different datasets, maintaining consistent model parameters across all experiments is a crucial prerequisite (i.e., the control variable method). Under this experimental design, any observed differences in simulation results are exclusively attributable to the variations in the input data. Therefore, we consider the current parameterization strategy sufficient to meet the requirements of this comparative analysis.

**3. Regarding dataset comparison:** We appreciate the reviewer's suggestion to include higher resolution or alternative datasets. In the revised manuscript, we have expanded the scope of comparison to include the MCD12Q1 PFT product, comparing it (alongside the ESA CCI PFT dataset) against the dataset reconstructed in this study. While we noted the reviewer's mention of the GLC\_FCS dataset, we selected MCD12Q1 because, like ESA CCI, it is one of the most widely used standard PFT forcing datasets within the dynamic global vegetation model (DGVM) community (Zhang et al., 2025; Xiao et al., 2025; Guan et al., 2023). The results (**Section 4.4, Page 25, Lines 576-646**) demonstrate that, compared to MCD12Q1 and ESA CCI, reductions in simulation errors for land surface carbon and water fluxes were observed across 63.1%–85.3% of the study area. We believe that benchmarking against these two products is sufficient to demonstrate the superiority of our reconstructed dataset over the prevailing global products currently used for carbon cycle modeling.

#### **References:**

Zhang, M., He, H., Zhang, L., Ren, X., Shi, L., Yu, G., Niu, Z., Qin, K., and Li, T.: Ecosystem engineering and global changes are increasingly enhancing China's terrestrial carbon sinks, *Resour.*

*Conserv. Recycl.*, 223, 108514, <https://doi.org/10.1016/j.resconrec.2025.108514>, 2025.

Xiao, C., Zaehle, S., Sitch, S., Duveiller, G., Pabon-Moreno, D. E., Walker, A. P., Knauer, J., Maignan, F., Schmulius, C., and Bastos, A.: Deforestation increases vegetation vulnerability to drought across biomes, *Glob. Biogeochem. Cycles*, 39, e2024GB008378, <https://doi.org/10.1029/2024GB008378>, 2025.

Guan, Q., Tang, J., Feng, L., Olin, S., and Schurgers, G.: Long-term changes of nitrogen leaching and the contributions of terrestrial nutrient sources to lake eutrophication dynamics on the Yangtze Plain of China, *Biogeosciences*, 20, 1635–1648, <https://doi.org/10.5194/bg-20-1635-2023>, 2023.

**[Specific Comment 1] Line 17:** The phrase “to accurately represent historical forest recovery, achieving an overall accuracy (OA)...” is misleading. The reported OA reflects the classification accuracy of forest cover rather than the ability to “represent historical recovery.”

**Response:** We appreciate your pointing this out. To avoid any misleading interpretation, we have revised **Lines 17–19** to explicitly state that the accuracy refers to the five aggregated types. The revised sentence reads as follows:

*“...Validation against independent data indicates that our reconstructed dataset achieves an overall accuracy (OA) of  $84.86\% \pm 1.18\%$  for five aggregated forest types (evergreen needleleaf forests, evergreen broadleaf forests, deciduous needleleaf forests, deciduous broadleaf forests, and mixed leaf forests)....”*

**[Specific Comment 2] Line 22:** The statement that the study “enhances the accuracy of evapotranspiration, leaf area index (LAI), and vegetation carbon flux by 49.4%-77%” is inaccurate. These values actually represent the proportion of China’s land area where simulation errors were reduced, rather than a direct measure of accuracy improvement. It is recommended to revise the sentence to: “reducing simulation errors for evapotranspiration, leaf area index (LAI), and vegetation carbon flux across 49.4%-77% of China’s land area...”

**Response:** We appreciate this suggestion. We have revised the sentence in **Lines 23–24** to read:

*“...reducing the simulation errors for evapotranspiration, leaf area index (LAI), and vegetation carbon flux across 63.1%–85.3% of China’s terrestrial area.”* Please note that the simulation results have been updated in the revised manuscript.

**[Specific Comment 3] Line 43:** Standardize the abbreviation for “land use and land cover change” to LUCC or LULC throughout the manuscript; remove inconsistent use of “LULC” when referring to change rather than land cover itself.

**Response:** We appreciate this correction. In the revised manuscript, we have standardized the abbreviation for “land use and land cover” as LULC. Accordingly, we have corrected all previous instances of “LUCC” to “LULC” throughout the text to ensure consistency.

**[Specific Comment 4] Line 46:** Specify the time period for terrestrial carbon storage estimates (e.g., 1980–2020 or 2000–2020) to avoid ambiguity.

**Response:** We appreciate you pointing this out. You are correct that the time period for the terrestrial carbon storage estimates in both studies is 1700–2000. To avoid ambiguity, we have revised **Lines 47–49** in the manuscript. The revised text reads as follows:

*“...it has led to three- to five-fold differences in estimates of China’s terrestrial carbon storage from similar bookkeeping models (e.g., 17–33 Pg C vs 6.18 Pg C from 1700 to 2000) (Houghton and Hackler, 2003; Ge et al., 2008).”*

#### **References:**

Ge, Q., Dai, J., He, F., Pan, Y., and Wang, M.: Land use changes and their relations with carbon cycles over the past 300 a in China, *Sci. China Ser. D Earth Sci.*, 51, 871–884, <https://doi.org/10.1007/s11430-008-0067-8>, 2008.

Houghton, R. A., and Hackler, J. L.: Sources and sinks of carbon from land-use change in China, *Global Biogeochem. Cy.*, 17, 1034, <https://doi.org/10.1029/2002GB001970>, 2003.

**[Specific Comment 5] Line 99:** When first mentioned, provide full names for abbreviations: GPP (Gross Primary Productivity), NEE (Net Ecosystem Exchange), and LAI (Leaf Area Index).

**Response:** We appreciate this correction. We have revised **Lines 101–102** in the manuscript to read: *“...namely gross primary production (GPP), net ecosystem exchange (NEE), leaf area index (LAI), and actual evapotranspiration (ET).”*

**[Specific Comment 6] Line 130:** Justify the use of the “nearest neighbor method” for resampling 30 m LULC data to 1 km. Explain why it was chosen over alternatives like bilinear interpolation, and

acknowledge potential uncertainties (e.g., preserving extreme values).

**Response:** We appreciate this valuable comment. In the revised manuscript, we have re-evaluated our resampling approach. We acknowledge that when downsampling from high resolution (30 m) to coarse resolution (1 km), the Nearest Neighbor method (which selects the pixel value closest to the centroid) can introduce significant uncertainty. However, we did not employ bilinear interpolation. Unlike continuous variables (e.g., temperature or elevation), Land Use and Land Cover (LULC) data consist of discrete categorical codes. Bilinear interpolation calculates weighted averages, which would generate non-existent or invalid class values (e.g., averaging class 1 and class 2 to result in 1.5). Consequently, bilinear interpolation is mathematically unsuitable for categorical LULC datasets. Therefore, we ultimately selected the majority (mode) method for resampling. This method assigns the value that appears most frequently within the target grid, ensuring that the resampled pixel represents the dominant land cover type of the area. This approach is widely recognized as the best standard practice for aggregating categorical LULC data. We have updated the description of the resampling method in **Page5, Line 135** to read:

*“...(ii) resampling to a 1 km resolution using the majority method...”*

Please note that due to this change in the resampling methodology, the statistical results presented in the revised manuscript and the newly uploaded dataset differ from those in the previous version.

**[Specific Comment 7] Line 132:** Clarify why Jeong’s NDVI dataset was selected instead of 1 km MODIS NDVI (2000–2023). The use of NDVI at 0.05° resolution has resulted in some coarse grid artifacts, particularly in the Qinghai-Tibet Plateau and northern Heilongjiang, in the data layer “China-ForestChange\_Gain\_Duration\_1km\_v1.0.tif.” The authors should explain why Jeong’s dataset was chosen despite these resolution limitations and discuss potential impacts on the results.

**Response:** We appreciate your constructive feedback regarding data quality. We acknowledge that, even with downsampling, the use of coarse-resolution NDVI data resulted in an inability to accurately capture fragmented forest edges and introduced “coarse grid artifacts” in the original dataset. Regarding the choice of data sources, MODIS NDVI data is only available from 2000 onwards, which fails to meet the requirements for reconstructing the historical periods of the 1980s and 1990s covered in our study (1981–2023). Unfortunately, no alternative NDVI datasets with a resolution higher than 1 km are currently available for the 1980s.

Consequently, in the revised manuscript, we adopted the “China 1985–2023 Annual Landsat Composite Dataset” published by Cai et al. (2025). This dataset integrates imagery from multiple Landsat sensors and addresses critical issues such as cloud and shadow contamination, reflectance consistency, and data gaps. Specifically, as this dataset employs a median composite method to aggregate all images within the growing season into a single annual image, we directly utilized the Red and Near-Infrared (NIR) bands to calculate the annual NDVI for the 1985–2023 period. Subsequently, we resampled these data from their native 30 m resolution to our target 1 km resolution using the mean method. Given the scarcity of Landsat imagery in the early 1980s, we used the 1985 data as a proxy for the 1981–1984 period. By adopting this higher-resolution dataset, the issue of coarse grid artifacts has been effectively resolved. We have revised **Section 2.3 (Page 5, Lines 137–147)** to align with our new input data.

**References:**

Cai, Y., Li, X., Zhu, P., Nie, S., Wang, C., Liu, X., and Chen, Y.: China Earth Observation Data Cube: The 30-m Seamless Annual Leaf-On Landsat Composites from 1985 to 2023, *J. Remote Sens.*, 5, 0698, <https://doi.org/10.34133/remotesensing.0698>, 2025.

**[Specific Comment 8] Line 155:** Justify the use of ERA5-Land (0.1° resolution) instead of higher-resolution Chinese climate datasets (e.g., Peng et al., 2019). Explain how potential biases were addressed.

**Response:** We agree with your point that high-resolution climate data is critical for accurately characterizing China’s complex eco-climatic features. Therefore, we have updated the climate dataset to use the data published by Peng et al. (2019). We have revised the corresponding text in **Page 6, Lines 161–164** of the revised manuscript:

*“...this study also utilised the 1 km resolution monthly mean temperature dataset for China (1981–2023) from Peng et al. (2019a). This dataset was generated by spatially downscaling the global 0.5° CRU climate dataset and the high-resolution WorldClim dataset using the Delta spatial downscaling method. The data are publicly available from the National Tibetan Plateau Data Center (<https://doi.org/10.11888/Meteoro.tpcdc.270961>, last access: 27 October 2025).”*

**References:**

Peng, S., Ding, Y., Liu, W., and Li, Z.: 1 km monthly temperature and precipitation dataset for China

from 1901 to 2017, *Earth Syst. Sci. Data*, 11, 1931–1946, <https://doi.org/10.5194/essd-11-1931-2019>, 2019a.

**[Specific Comment 9] Line 182:** Correct the inconsistency in Figure S1 (Chongqing subfigure), where the sum of broadleaf and needleleaf forest area does not equal total forest area pre-2002.

**Response:** In the National Forest Inventory (NFI), the “total forest area” comprises needleleaf forests, broadleaf forests, bamboo forests, economic forests, and shrublands (**detailed in Section 3.1, Page 7, Lines 179–195**); consequently, there is a discrepancy between the sum of needleleaf/broadleaf forest areas and the total forest area reported in the NFI.

In the revised manuscript, we adopted “wooded land” as the area constraint. This strategy effectively mitigates the potential interference of shrublands on forest identification and ensures that the sum of our reconstructed needleleaf and broadleaf areas aligns more closely with the target forest area (**Fig. 5**).

Accordingly, we have removed the original Figure S1 and replaced it with figures illustrating the area reconstruction process for “wooded land” and “arbor forest” (**Revised Figs. S1 and S2**). We have also updated **Sections 3.1 and 3.2 (Page 7, Lines 179–226)** of the Methods to provide a systematic description of this process.

**[Specific Comment 10] Line 228:** Explicitly list the seven LULC products used for PFTs classification in Table S1 (dataset names, years, sources).

**Response:** We appreciate this suggestion. In the revised Table S1, we have employed the labels “a”, “b”, and “c” to categorize the products used for forest reconstruction and PFT classification. Specifically, the label “b” denotes the datasets utilized for PFT classification (where we provided details on dataset names, years, and sources).

Please note that in the revised manuscript, the number of LULC products used for PFT classification has increased from 7 to 9. This expansion resulted in a total of 92 data layers for the consistency grade maps of needleleaf and broadleaf forests (**Fig. S5**), compared to 73 layers in the original version. Consequently, this increased data density contributes to more robust PFT classification results.

**Table S1.** Land use and land cover (LULC) datasets used in this study.

---

| <i>Datasets</i> | <i>Resolution</i> | <i>Time range</i> | <i>Data source</i> |
|-----------------|-------------------|-------------------|--------------------|
|-----------------|-------------------|-------------------|--------------------|

---

|                                     |           |                     |   |
|-------------------------------------|-----------|---------------------|---|
| <i>CLCD</i> <sup>a,c</sup>          | 30 m      | 1980s–2023          | (Yang and Huang, 2021)  |
| <i>CNLUCC</i> <sup>a,c</sup>        | 30 m/1 km | 1980–2023           | <a href="http://www.resdc.cn">http://www.resdc.cn</a>   |
| <i>CGLS</i> <sup>b,c</sup>          | 100 m     | 2015–2019           | (Buchhorn et al., 2020)   |
| <i>ESA_CCI</i> <sup>b,c</sup>       | 300 m     | 1992–2020           | <a href="https://data.ceda.ac.uk/neodc/esacci/land_cover/data">https://data.ceda.ac.uk/neodc/esacci/land_cover/data</a> |
| <i>GLC_FCS30D</i> <sup>b,c</sup>    | 30 m      | 1985–2022           | (Zhang et al., 2024)  |
| <i>GFC30</i> <sup>a</sup>           | 30 m      | 2018                | (Zhang et al., 2020)  |
| <i>GLC2000</i> <sup>b</sup>         | 1 km      | 2000                | (Bartholomé and Belward, 2005)  |
| <i>GLCNMO</i> <sup>b</sup>          | 1 km      | 2003, 2008,<br>2013 | (Tateishi et al., 2011)   |
| <i>GlobeLand30</i> <sup>a</sup>     | 30 m      | 2000, 2010,<br>2020 | (Chen et al., 2015)   |
| <i>GlobCover</i> <sup>b</sup>       | 300 m     | 2005, 2009          | (Bontemps et al., 2011)   |
| <i>FROM_GLC</i> <sup>a</sup>        | 10 m      | 2017                | (Gong et al., 2019)   |
| <i>MLUD</i> <sup>a</sup>            | 250 m     | 2005                | (Ge et al., 2018)   |
| <i>Wu_LC</i> <sup>a</sup>           | 1 km      | 1980s               | <a href="http://www.resdc.cn">http://www.resdc.cn</a>   |
| <i>MCD12Q1</i> <sup>b,c</sup>       | 500 m     | 2001–2023           | (Sulla-Menashe et al., 2019)  |
| <i>ESA_WorldCover</i> <sup>a</sup>  | 10 m      | 2021, 2022          | <a href="https://esa-worldcover.org/en">https://esa-worldcover.org/en</a>   |
| <i>Hansen</i> <sup>a</sup>          | 30 m      | 2000–2012           | (Hansen et al., 2013)   |
| <i>JRC_ForestTypes</i> <sup>a</sup> | 10 m      | 2020                | (Bourgoin et al., 2025)   |
| <i>GFCH</i> <sup>a</sup>            | 30 m      | 2019                | (Potapov et al., 2021)  |
| <i>IGBP DISCover</i> <sup>b</sup>   | 1 km      | 1992–1993           | (Loveland et al., 1999)   |
| <i>MiCLCover</i> <sup>b</sup>       | 1 km      | 2000                | (Ran et al., 2009)  |
| <i>TCC</i> <sup>a</sup>             | 30 m      | 2010                | <a href="https://glad.umd.edu/Potapov/TCC_2010/">https://glad.umd.edu/Potapov/TCC_2010/</a>                             |
| <i>CLUD-A</i> <sup>a,c</sup>        | 1 km      | 1981–2023           | (Xu et al., 2020)   |

<sup>a</sup>. These datasets delineate a single, general forest category and lack classification into specific subtypes.

<sup>b</sup>. These datasets provide detailed classifications of various forest subtypes and were used for the plant functional types (PFTs) classification in this study.

<sup>c</sup>. These datasets are updated on an annual basis, in contrast to others which are produced only for specific years.

**[Specific Comment 11] Line 301:** Justify why a 10 km × 10 km window size was used for neighborhood analysis.

**Response:** We appreciate this comment. The selection of a 10 km × 10 km window size for the neighbourhood analysis was made with reference to previous studies such as Harper et al. (2023), who employed a comparable analytical scale (0.25° × 0.25°). Our 10 km × 10 km window corresponds to approximately 0.1°, which is finer than the 0.25° scale used in the referenced study. Furthermore, this size aligns perfectly with the simulation resolution (0.1°) of the LPJ-GUESS model used in the subsequent stages of our research. Consequently, we consider this window size to be methodologically reasonable and appropriate. We have added the corresponding description on **Page 12, Line 336**, which reads:

*“For each “residual” pixel, a 10×10 pixel neighbourhood window was established, a size selected with reference to previous studies performing neighbourhood analysis at similar scales (Harper et al., 2023).”*

**References:**

Harper, K. L., Lamarche, C., Hartley, A., Peylin, P., Otlé, C., Bastrikov, V., San Martín, R., Bohnenstengel, S. I., Kirches, G., and Boettcher, M.: A 29-year time series of annual 300 m resolution plant-functional-type maps for climate models, *Earth Syst. Sci. Data*, 15, 1465–1499, <https://doi.org/10.5194/essd-15-1465-2023>, 2023.

**[Specific Comment 12] Line 327:** Correct the claim that ERA5-Land daily temperature data are unavailable. Daily data are accessible via Google Earth Engine and Copernicus Climate Data Store.

**Response:** We appreciate this correction. In the revised manuscript, we have adopted the monthly mean temperature dataset published by Peng et al. (2019) instead of using ERA5-Land data. Consequently, the incorrect statement regarding the availability of ERA5-Land daily data has been removed from the text.

**[Specific Comment 13] Line 361:** Using three years as a threshold to identify the stable forest is not reasonable for forest land due to its longer growth period (e.g., 5-10 years) compared with cropland.

**Response:** We appreciate this suggestion and agree with your point. In the revised manuscript, we have adopted a five-year threshold to identify stable forests. Accordingly, we have revised the text in **Page 15, Line 422** and have redrawn **Figure 6**.

*“...For this analysis, a “stable” forest state was defined as a pixel remaining as forest for at least five consecutive years...”*

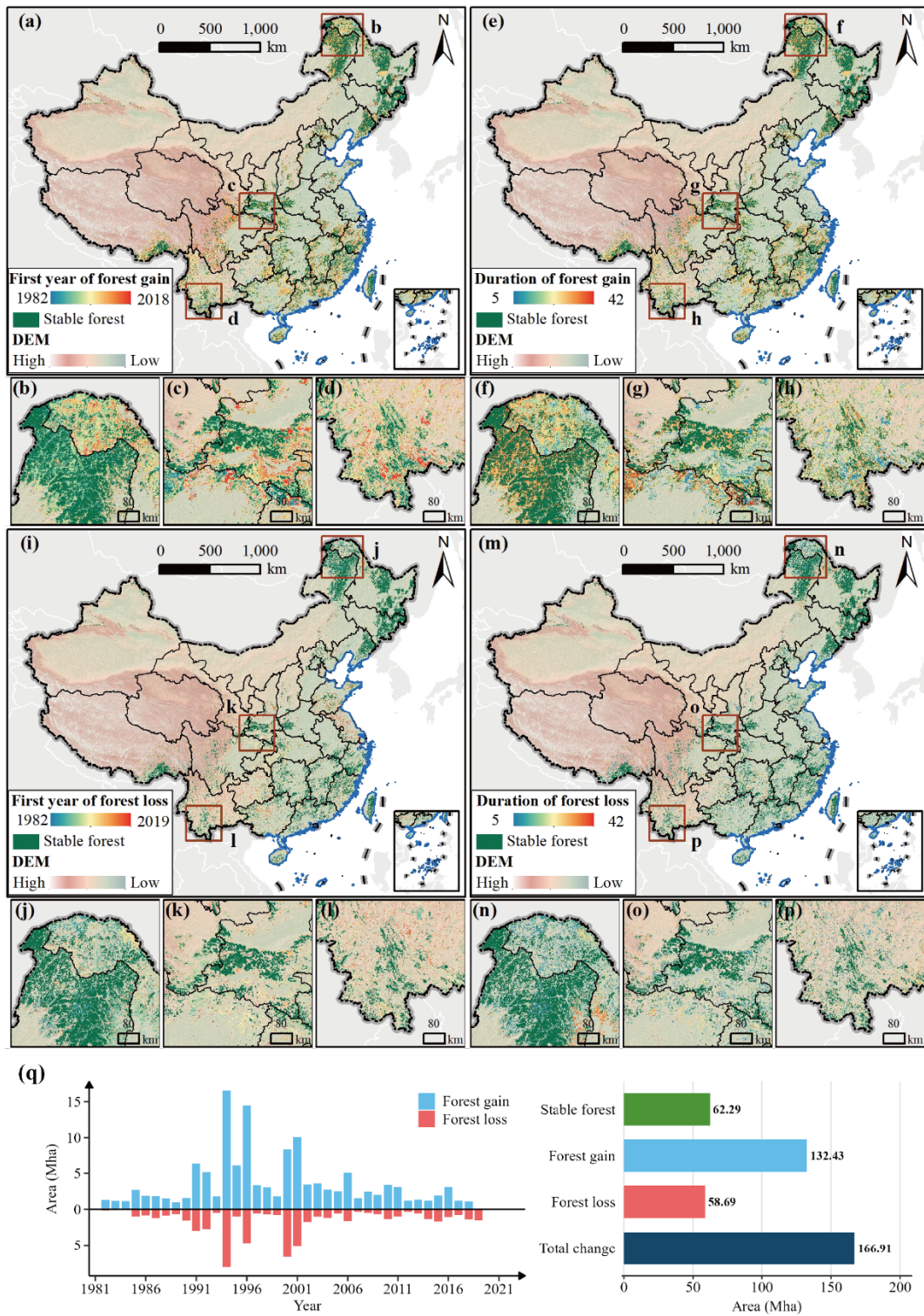


Figure 6. Spatiotemporal dynamics of forest gain and loss in China from 1981 to 2023. This figure presents: (a-h) the spatial patterns of forest gain, showing onset year and duration; (i-p) the spatial patterns of forest loss; and (q) the national-scale temporal dynamics, including the annual areas of forest gain and loss and a summary of total stable, gained, and lost forest areas.

**[Specific Comment 14] Line 320-325:** Four plant functional types were further classified using GDD and temperature followed the method of Bonan et al. (2002). Clarify annual GDD or multi-year mean GDD was used when conduct the final PFTs classification. Additionally, the GDD data can be improved by using high spatial and temporal resolution temperature dataset.

**Response:** We appreciate this correction. We confirm that we utilized annual Growing Degree Days (GDD) for the final PFT classification. To improve the accuracy of these GDD estimates, we adopted the dataset published by Peng et al. (2019). We selected this dataset because its 1 km spatial resolution aligns perfectly with our PFT mapping scale, allowing for a more refined representation of local thermal conditions compared to coarser global products. We have revised the description of this process in **Page 13, Lines 363–367** of the revised manuscript:

*“Since we used the monthly mean temperature data for 1981–2023 published by Peng et al. (2019a), an alternative method was employed to estimate GDD. This involved substituting the monthly mean temperature for  $T_a$  in Eq. (4) and then multiplying the result by the number of days in that month to yield a monthly GDD value. The annual GDD was subsequently calculated as the sum of these monthly values. We utilised the annual GDD and  $T_c$  values for each year during the 1981–2023 period to reflect the year-to-year dynamic changes in climatic conditions.”*

**[Specific Comment 15] Lines 394–395:** Cite the corresponding table or figure for the reported percentages (6.9% needleleaf, 2.7% broadleaf forest pixels) to support the claim.

**Response:** We appreciate this suggestion. We have produced **Supplementary Figure 8 (Fig. S8)** to support the reported percentages (please note that these percentages have been updated in the revised manuscript) and have revised the relevant description on **Page 17, Line 480**.

*“Furthermore, according to our methodology, a pixel-weighted average over the 1981–2023 period indicates that fewer than 1% of pixels for all five reconstructed PFT types did not fall within their corresponding consistency type (the specific proportions were 0.50% for DBF, 0.10% for EBF, 0.03% for DNF, 0.01% for ENF, and 0.05% for MF, Fig. S8).”*

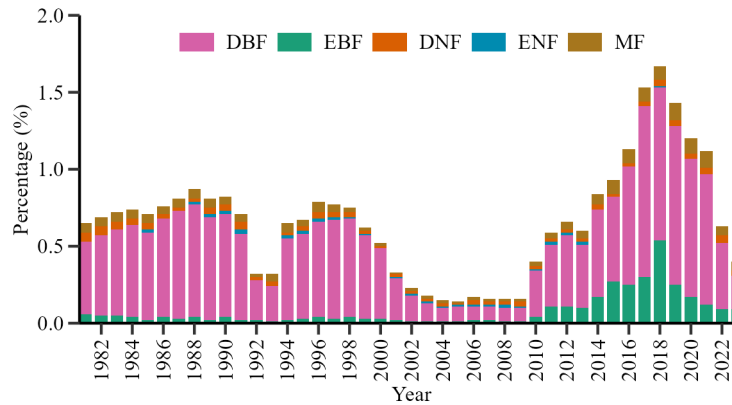


**Figure S8.** Percentage of pixels for the five reconstructed plant functional types (PFTs) not falling within their corresponding consistency type, 1981–2023. DBF: deciduous broadleaf forest, EBF: evergreen broadleaf forest, DNF: deciduous needleleaf forest, ENF: evergreen needleleaf forest, MF: mixed leaf forest.

**[Specific Comment 16] Lines 425–430:** Relocate the description of PFTs dataset availability from the “Reconstructed Forest Cover Dataset Description” section to a dedicated “Data Availability” section.

**Response:** We appreciate this suggestion. We have moved the description regarding the availability of the PFT dataset to the “Data Availability” section (**Page31, Line 725**). Please note that the DOI of the dataset has been updated in the revised version.

*“The reconstructed forest cover dataset generated in this study is publicly available in the Zenodo repository at <https://doi.org/10.5281/zenodo.17656153> (Liu et al., 2025).”*

**[Specific Comment 17] Figure 4:** Remove “Bamboo and Economic forest” from the PFTs legend, as it is not included in the 8-class PFTs classification.

**Response:** We appreciate this suggestion. In the revised manuscript, we have removed the “bamboo and economic forest” categories from Figure 4 and added the “mixed leaf forest” category. Please note that the “mixed leaf forest” class is not merely a substitution for the removed categories; rather, it was derived using a completely new extraction logic (**detailed in Section 3.4.2, Page11, Lines 314–352**).

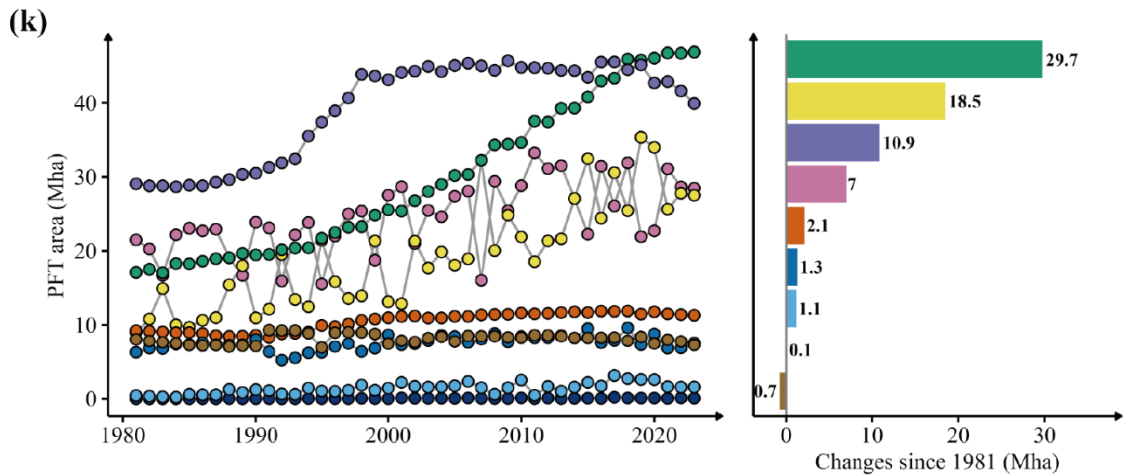
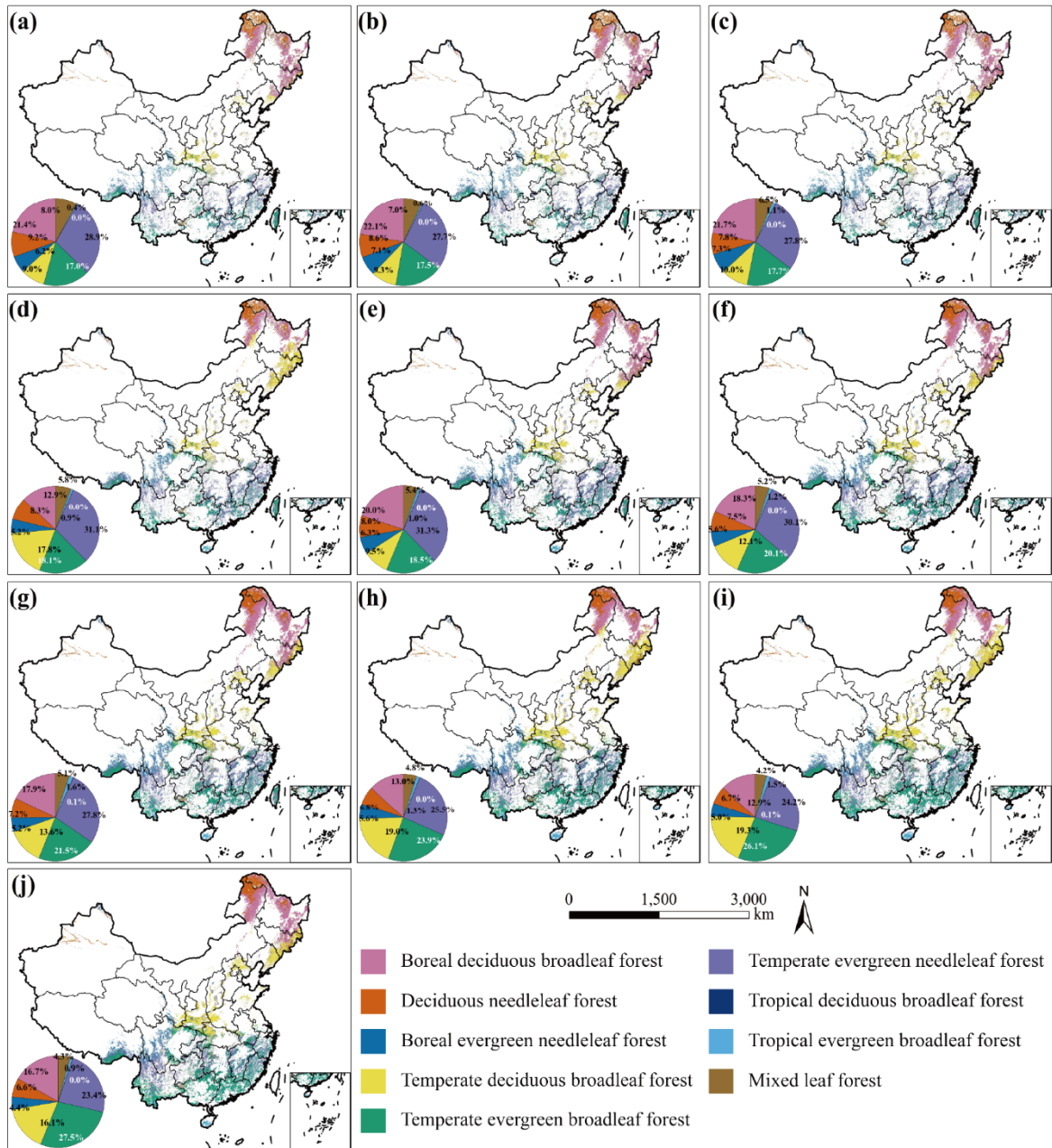


**Figure 4.** Spatial distribution patterns and area proportions of China’s forest plant functional types (PFTs) for selected years between 1981 and 2023, (a)-(j) correspond to the years 1981, 1985, 1990, 1995, 2000, 2005, 2010, 2015, 2020, and 2023, respectively; (k) Temporal dynamics and total variation in PFTs from 1981 to 2023.

**[Specific Comment 18] Figure 5:** Correct numerical and unit errors: Verify the unrealistic forest area values for GLASS\_GLC, CGLS, ESA\_WorldCover and GLCNMO (~6,000,000 km<sup>2</sup>). Ensure the sum of needleleaf and broadleaf forest area matches total forest area for GLC\_FCS, MODIS, and GLCNMO. Standardize units across figure and caption (e.g., 10<sup>6</sup> ha or km<sup>2</sup>).

**Response:** We sincerely apologize for this oversight. In our previous calculations of total forest, needleleaf, and broadleaf areas, we utilized the resampled data, which resulted in an overestimation of the forest area. In the revised manuscript, we have recalculated these figures using the original data (at native resolution). We found that the forest area in the GLC\_FCS30D dataset ranges from 232 to 238 million hectares (Mha) for the period 1985–2022, with a total area of 234 Mha in 2010. We performed similar recalculations for all other datasets and ensured that the sum of needleleaf and broadleaf forest areas aligns with the total forest area. Accordingly, we have revised Figure 5 and standardized the units in all figures and captions to “Mha”.

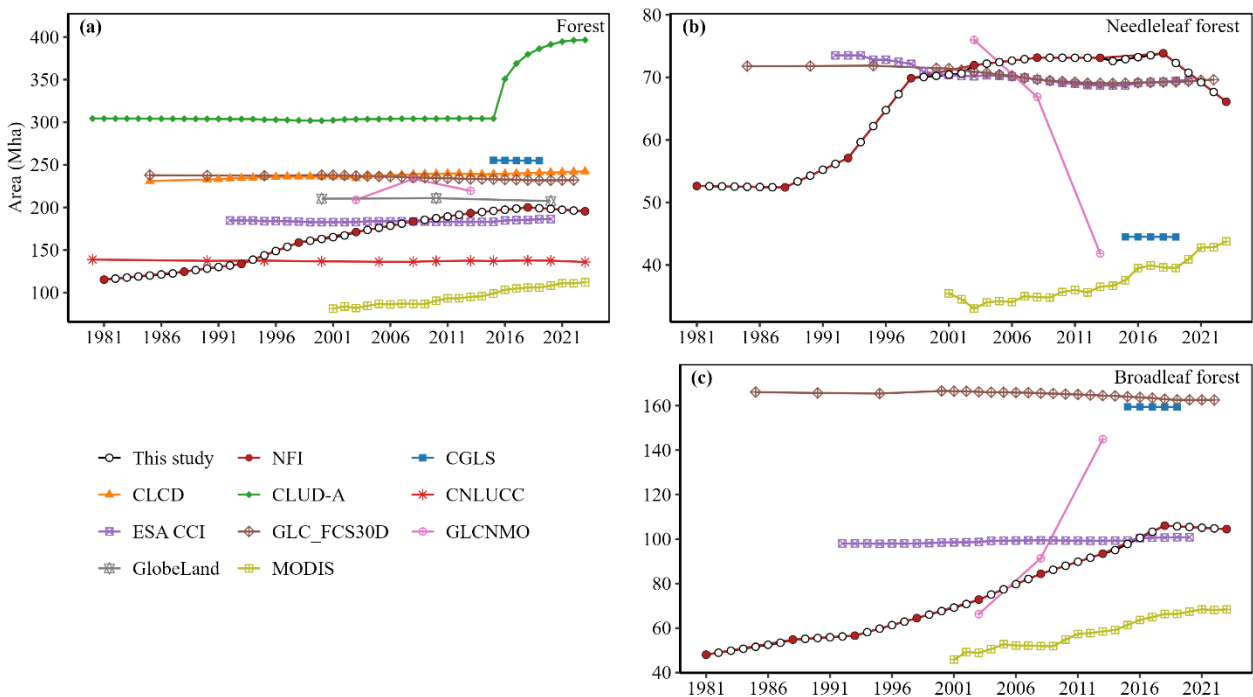


**Figure 5.** Temporal dynamics of national-scale total forest area, comparing the results of this study

*with data from national forest inventory (NFI) and other selected land use and land cover (LULC) products: (a) forest, (b) needleleaf forest, and (c) broadleaf forest.*

**[Specific Comment 19] Figure 6:** Explain the high forest loss on the Qinghai-Tibet Plateau in recent years. Discuss potential causes such as natural disturbances (permafrost thaw), human activities (infrastructure), or classification errors.

**Response:** We appreciate this suggestion. We have conducted an in-depth analysis of the forest loss observed in the Qinghai-Tibet Plateau by combining historical policy contexts and relevant literature. In the revised manuscript, we have clarified the specific timing and drivers of this change. We identified that the severe forest loss was primarily concentrated in the eastern Qinghai-Tibet Plateau during the period of 1990–1996. Existing studies (e.g., Chen et al., 2013) confirm that the loss during this period was primarily driven by commercial logging. Furthermore, following the implementation of large-scale ecological restoration programs initiated in 1998—specifically the Natural Forest Protection Program and the Grain for Green Program—forest cover in this region exhibited a distinct recovery trend from 2000 to 2008 (Liu et al., 2008). We have added relevant content to the revised manuscript (**Page 23, Lines 556–559**) to explain the potential causes of forest dynamics in this region. *“We identified severe forest loss in the eastern Qinghai-Tibet Plateau during 1990–1996, which appears to be primarily driven by commercial logging (Chen et al., 2013). Following the implementation of large-scale ecological restoration programmes initiated in 1998—specifically the Natural Forest Protection Programme and the Grain for Green Programme—forest cover exhibited a recovery trend from 2000 to 2008 (Liu et al., 2008).”*

**References:**

Chen, H., Zhu, Q., Peng, C., Wu, N., Wang, Y., Fang, X., Gao, Y., Zhu, D., Yang, G., and Tian, J.: The impacts of climate change and human activities on biogeochemical cycles on the Qinghai-Tibetan Plateau, *Glob. Change Biol.*, 19, 2940–2955, <https://doi.org/10.1111/gcb.12277>, 2013.

Liu, J., Li, S., Ouyang, Z., Tam, C., and Chen, X.: Ecological and socioeconomic effects of China's policies for ecosystem services, *Proc. Natl. Acad. Sci. U.S.A.*, 105, 9477–9482, <https://doi.org/10.1073/pnas.0706436105>, 2008.

**[Specific Comment 20]** Data comparisons between this study and Xia et al. (2023) should also be

included in the analysis or discussion section.

**Response:** We appreciate this suggestion. As elaborated in our response to Comment #1 of the “Major Comments” section above, we have provided a detailed comparison between our study and the work of Xia et al. (2023). Accordingly, we have added a dedicated comparative analysis to the Discussion section of the revised manuscript, which specifically examines the potential reasons for the observed discrepancies between the two datasets. This relevant discussion is presented in **Page29–30, Lines 663–672:**

*“Notably, while both this study and Xia et al. (2023) aimed to reconstruct forest growth trends consistent with NFI records, certain discrepancies exist in the results. For instance, Xia et al. (2023) identified low forest classification consistency primarily in the northwestern regions of Xinjiang, Qinghai, and Ningxia, whereas our study observed low consistency solely in Ningxia. This divergence likely stems from our adoption of a stricter NFI area constraint—specifically, utilising ‘wooded land’ (excluding shrubland) rather than total forest area. By excluding shrublands, our extracted distribution of ‘potential forest’ aligns more closely with the actual forest distribution in sparsely forested regions such as Xinjiang and Qinghai. Furthermore, a comparison of data between 1990 and 1995 by Xia et al. (2023) suggested a relatively low area of forest loss in China during this period. In contrast, our dataset reveals the opposite trend, identifying a peak in forest loss between 1991 and 1994. This difference is likely attributable to the annual temporal resolution of our dataset, which offers heightened sensitivity to forest gain and loss events.”*

**References:**

Xia, X., Xia, J., Chen, X., Fan, L., Liu, S., Qin, Y., Qin, Z., Xiao, X., Xu, W., and Yue, C.:  
Reconstructing long-term forest cover in China by fusing national forest inventory and 20 land use and land cover data sets, *J. Geophys. Res.-Biogeo.*, 128, e2022JG007101, <https://doi.org/10.1029/2022JG007101>, 2023.

**[Specific Comment 21]** All figure captions use “Figure \*,” but in the main text the figures are cited as “Fig. \*.”

**Response:** We appreciate this observation. We have consulted the Copernicus Publications Author Guidelines and reviewed several relevant papers published in ESSD (e.g., Yang and Huang, 2021; Zhang et al., 2024). We found that according to the journal’s standard format, the abbreviation “Fig.”

is required for in-text citations, while “Figure” is used in figure captions. Therefore, to comply with the journal’s standard formatting requirements, we have retained the usage of “Fig.” in the main text.

### **References:**

Yang, J., and Huang, X.: 30 m annual land cover and its dynamics in China from 1990 to 2019, *Earth Syst. Sci. Data*, 13, 2021–2039, <https://doi.org/10.5194/essd-13-2021-2021>, 2021.

Zhang, X., Zhao, T., Xu, H., Liu, W., Wang, J., Chen, X., and Liu, L.: GLC\_FCS30D: the first global 30 m land-cover dynamics monitoring product with a fine classification system for the period from 1985 to 2022 generated using dense-time-series Landsat imagery and the continuous change-detection method, *Earth Syst. Sci. Data.*, 16, 1353–1381, <https://doi.org/10.5194/essd-16-1353-2024>, 2024.

We appreciate your warm work earnestly, and hope that the correction will meet with approval. We tried our best to improve the manuscript and made some changes in the manuscript. These changes will not influence the content and framework of the paper. And here we did not list the changes but marked in **red** in revised paper.

**Once again, thank you very much for your comments and suggestions.**